Light Metals 2016
Edited by: Edward Williams
TMS (The Minerals, Metals & Materials Society), 2016

HIGH TEMPERATURE CREEP EVOLUTION IN Al-Si ALLOYS DEVELOPED FOR AUTOMOTIVE POWERTRAIN APPLICATIONS: A NEUTRON *IN-SITU* STUDY ON *HKL*-PLANE CREEP RESPONSE

Dimitry G. Sediako[1], Wojciech Kasprzak[2], Frank Czerwinski[2],
Ahmed M. Nabawy[1], and Amir R. Farkoosh[3]

[1]Canadian Neutron Beam Centre, Canadian Nuclear Laboratories, Chalk River, ON, Canada
[2]CanmetMATERIALS, Hamilton, ON, Canada
[3]McGill University, Montreal, QC, Canada

Keywords: Aluminum alloy, automotive powertrain, high temperature creep, neutron diffraction

Abstract

Recent trend in the automotive industry towards lightweighting and downsizing the powertrain components, without compromising the power output, have led to increased engine power density. Increased power density frequently requires these lighter components to operate in conditions of increased temperature and pressure, which is challenging for many aluminum alloys in use today in the powertrain manufacturing. Meeting the challenge requires not only improving high-temperature performance of known alloys or developing new ones, but also developing new advanced techniques to understand the long-term behaviour of the alloys.

This *in-situ* neutron diffraction study evaluated creep strain for individual *hkl* planes in three automotive alloys under tensile load. The conditions of temperature and pressure were typical of or similar to those experienced by engine heads in service. High temperature plastic and elastic creep properties of three cast aluminum alloys were characterized. The properties determined for these alloys can be used as a benchmark for further development of advanced alloy systems suitable for the engine head application.

The *in-situ* neutron diffraction measurements provided data on d-spacing evolution for various *hkl* crystallographic planes as a function of temperature, tensile load, and time; thereby revealing *hkl*-specific evolution of elastic strains. This information contributes to in-depth understanding of why a particular alloy exhibits particular service properties (eg. creep).

Introduction

Characteristics of the primary creep regime, including the initial strain required before the onset of creep, the strain hardening characteristic that retards the rate of creep up to the steady state secondary creep regime can all be used to determine the quality of an alloy and help predict the long term behavior. This kind of information becomes extremely valuable in selecting/developing alloys for the most critical applications in automotive powertrain, for example, cylinder heads.

Significant improvements in fuel economy and powertrain weight can be achieved by enhancing engine efficiency and through replacement of large engines by smaller ones in the same vehicle class. Weight reduction potential by reduced engine size is also increased by the ability to reduce the engine support structure, allowing further weight reductions.

In a simulation of a diesel engine, a 60% increase in power and torque requires increase in maximum cylinder head pressure from 18 MPa to 30 MPa, increase in peak head temperature from 215 to 275^{o}C and from 150 to 190^{o}C on the head combustion face and water jacket face respectively. Authors [1] studied a 6-cylinder turbo medium duty diesel engine and reported that temperature distribution across the cylinder head deck face is ranging from 200 to 350^{o}C, while typical temperatures for the valves and injector regions are 250~260^{o}C. These service parameters (high temperatures and increased pressures) are very challenging for aluminum alloys currently used in engine applications. To achieve the future 2017-2025 industry-mandatory Corporate Average Fuel Economy (CAFE) targets, significant technological changes of engine materials are required.

The objective of this study is to develop a basis for identification of a cast aluminum alloy with improved high temperature properties, including creep and high cycle fatigue strength over the potential service life of the engine. The expected running life of an engine is between 2000 and 4000 hours. Such long term testing is both very expensive and time prohibitive to enable comprehensive evaluation of an alloy. A study of the creep behavior, including the primary and secondary creep regions, and identifying the transition point, will help identify the alloy chemistry and processing conditions that are capable of sustaining the thermal mechanical loads over the expected life cycle of an engine.

Experimental

Sample material

Three different aluminum alloys were cast in ASTM B108 steel mold and then used to machine the 80-mm-long creep specimens, as shown in Figure 1. The specimens were machined from the “gauge” section of the cast test bar.

Table 1 represents the typical chemical composition of the three alloys investigated. The well-known commercial A380 material was produced as a reference point for the “base” and “new” material performance evaluation. The principal difference between the two Al-7wt%Si alloys is the addition Zr, Ti, and V into the alloy with the designation “new”.

Table I
Chemical Composition of the alloys under investigation.

Alloy	Alloying Elements (Wt%)									
	Si	Cu	Mg	Fe	Sr	Mn	Zr	Ti	V	Al
A380	9.5	3.4	0.071	0.90	<0.001	0.19	0.007	<0.001	0.009	Bal.
"Base"	7.1	1.02	0.50	0.090	0.0086	0.005	-	-	-	Bal.
"New"	7.02	0.95	0.48	0.090	0.012	0.005	0.56	0.20	0.32	Bal.

Figure 1. The aluminum test bar (*a*.) cast using ASTM B108 steel mold and machined creep specimen (*b*.). Total length of the specimen is 80 mm, with the length of the gauge section of 32 mm.

Neutron Diffraction: In-Situ Creep Strain Measurements

The creep strain measurements were performed at L3 neutron diffractometer of the Canadian Neutron Beam Center (CNBC), Canadian Nuclear Laboratories, in Chalk River, ON, Canada. A detailed description of the testing procedure was published earlier in [2-5]. Elastic strain (ε) of the atomic lattice was measured using the peak shift method. This method calculates strain using the change in lattice spacing:

$$\varepsilon = {(d_0 - d)}/{d_0} \quad (1)$$

Where d_0 and d are the lattice spacing before and after creep, respectively. The lattice spacing was calculated using Bragg's law:

$$n\lambda = 2dsin(\theta) \quad (2)$$

Where λ is the neutron wavelength (1.55 Å), n=1 for the first order diffraction, and θ is the neutron scattering angle measured during the neutron diffraction experiment.

The elastic strains were measured in the direction parallel to the applied load for several crystallographic planes: (111), (311), (200), and (220). The neutron-diffraction experimental setup, shown in Figure 2, includes a high-temperature extensometer that measures the total value of strain (both plastic and elastic components).

Experiment Procedure and Selection of Experimental Parameters

One of the objectives of this study was evaluation of the elastic/plastic tensile primary-and-secondary creep properties near the yield strength of the material because critical areas of the automotive engine are often operated near these limits. As mentioned earlier, the temperature requirements for aluminum alloys in the automotive industry have increased and will increase further, therefore the test data are now frequently collected at higher temperatures. In this study the analysis was focused on the primary and secondary creep behavior at 200°C and 250°C, as oppose to the typical for earlier studies range of 150-175°C as aluminum was rarely used for the higher-temperature applications.

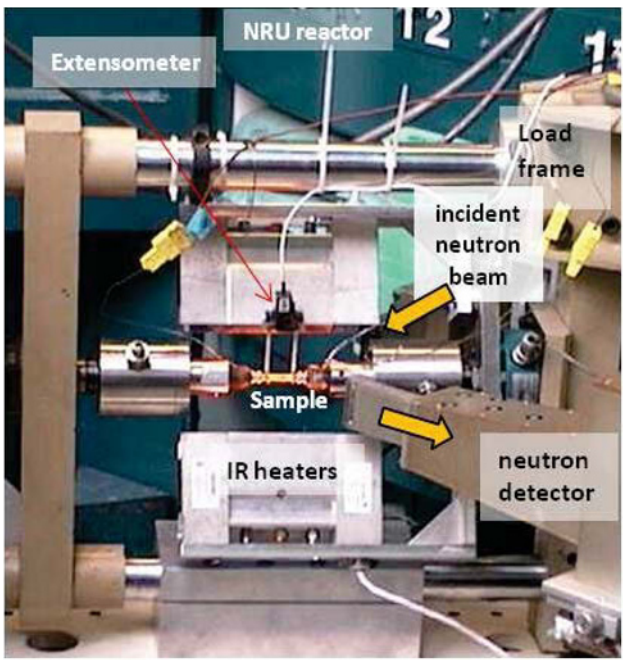

Figure 2. Experimental setup: In-situ neutron diffraction measurement of strain evolution in high-temperature tensile creep.

The procedure for the neutron experiment included the following:

- Sample "conditioning" at the experiment temperature for 200 hours prior to the experiment;
- Upon installation of the sample at the neutron diffractometer (Fig. 2), heating the sample to the experiment temperature (either 200 or 250°C) and measuring the diffraction angles for the selected *hkl* planes (for calculating the corresponding values of *d*-spacing, equation /2/), prior to applying the tensile load. These no-load values for the *d*-spacing are later used as a reference in calculation of the induced strains (equation /1/).
- Applying the tensile load, initially at ~90% of the yield strength, and maintaining it for as long as it takes for the

creep to enter the steady-state region (the secondary creep phase) and exhibit the constant creep rate for at least 14~16 hours, while continuously measuring the angular peak position for the selected neutron diffraction planes.

- Releasing the applied load and measuring the new diffraction peaks' positions, therefore determining the new reference value of *d*-spacing for the strain calculation (if the value is different from the original).
- Adding ~10% to the original tensile load value and applying this load to the sample. Again, maintaining the new load value, allowing the sample exhibit the steady-state creep for at least 14-16 hours. Continuously measuring the angular position for the selected neutron diffraction peaks.
- Releasing the applied load and measuring the new no-load diffraction peaks' positions.
- Continuing the above steps while adding 10% to the value of the applied tensile load until the eventual sample fracture.
- Continuously recording the total over-all strain, thermal+plastic+elastic, throughout the experiment.

In the technical literature there are several available sets of tensile properties of the A380 alloy tested at various temperatures. For example, tensile properties of die cast alloy A380 have been measured [6] and are listed in Table II. The listed values for yield strength at 200 and 250^{0}C were used in determining the initial load values, as per the experiment procedure outlined above. This starting load values are presented in Table III.

Table II
Tensile properties of die cast alloy A380 at various temperatures [6]

Temperature (C)	Tensile Strength (MPa)	Yield Strength (MPa)	Elongation (%)
150	235	152	5
205	165	110	8
260	90	55	20

Table III
"Starting" experimental parameters

Temperature (C)	Initial Operating Load (MPa)
200	90
250	72

Results and Discussion

Experimental results

The experimental results are presented in Figures 3 and 4. The data show that the elastic strains developed at different crystallographic planes vary with respect to load, temperature, and alloy compositions. These variations can be linked to the creep properties of the alloys under investigation enabling a better understanding of the service performance of these alloys in the automotive powertrain applications.

As presented in Figure 3, at the lower test temperature of 200^{o}C, the (111) crystallographic planes, typically followed by the (311) planes, have the highest level of elastic strains compared to the (200) and (220) planes. An exception to this trend is found in A380 alloy at the second loading stage, where the (220) planes show an increased level of strains similar to those obtained for the (111) and (311) planes.

However, as the testing temperature increased to 250^{o}C (Figure 4), the strains developed at (200) and (220) planes increase greatly, in some cases being at par or even exceeding those obtained for the (111), and (311) planes.

The "base" alloy performance at 200^{o}C was comparable to the other two alloys, but as the temperature increased to 250^{o}C the initial load setting had to be reduced to 45 MPa for this alloys, while maintaining the initial load setting of 72 MPa for the other two alloys. This was due to significantly reduced material strength that led to pronounced elongation of the sample; this sample failed shortly after the load reached 54.5 MPa, while the A380 alloy was still tested at 80 MPa, and the "new" alloy sample reached 88 MPa before failing.

Analysis of the total (thermal+plastic+elastic) creep strains and strain rates exhibited by the three alloys at different experiment conditions allowed for calculations of the power-law stress exponent, further used in the analysis of the creep mechanisms.

Creep Mechanism

According to the calculations of homologous temperatures, T_m/T (T_m: melting temperature of alloy; T: test temperature of 200-250^{o}C), and normalized stresses, σ/G (σ: applied stress of 45-130MPa; G: shear modulus of 27GPa). The normalized stresses for the alloys under investigation are located in the range of 2.2~2.9 $\times 10^{-3}$ for the applied stress of 45 MPa to 5×10^{-3} for the applied stress of 130 MPa. Thus the main suggested creep mechanism is dislocation creep, which is dominant at normalized stress range of $10^{-4} < \sigma/G < 10^{-2}$ [2].

Deformation mechanism map developed in an earlier study [3] for pure aluminum is shown in Figure 5. The normalized stress here, σ/G, is plotted versus homologous temperature, T_m/T, in order to represent the different creep mechanisms with respect to temperature and applied stress level. The creep mechanisms are presented for the range of temperatures from a high of $T=T_m$ (T_m/T=1) to a low of less than $0.2T_m$ (T_m/T=5). The region applicable to our test conditions is highlighted in this figure. It follows that for pure aluminum the imposed conditions would cause the power-law breakdown (PLB) creep mode, bordering with dislocation creep on one side and pure plasticity on the other.

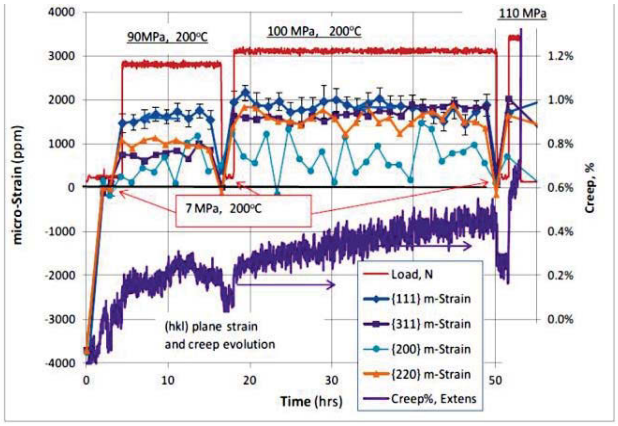

(a)

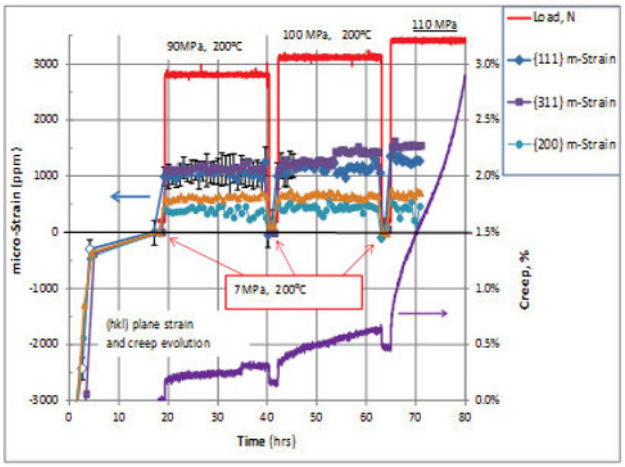

(b)

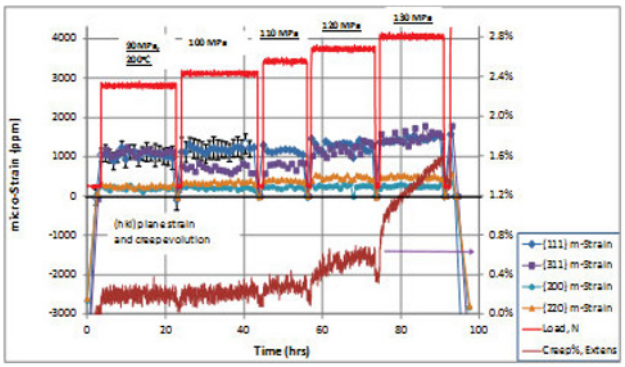

(c)

Figure 3. Creep strain (%) and elastic microstrain (ppm) evolution at elected *hkl* planes at 200°C during ascending cyclic loading for A380 alloy (a), "base" alloy (b), and "new" alloy (c)

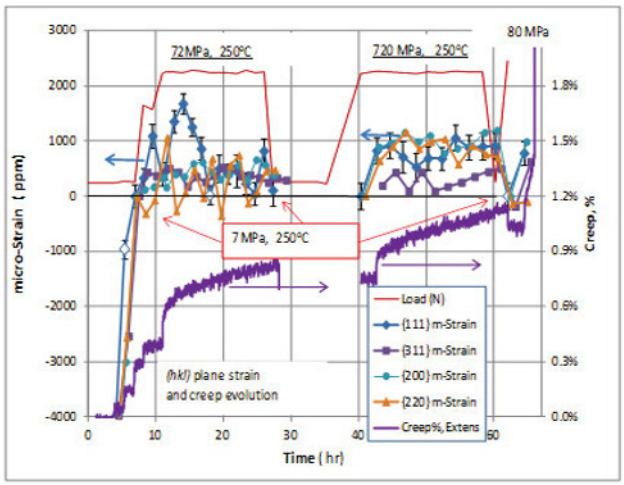

(a)

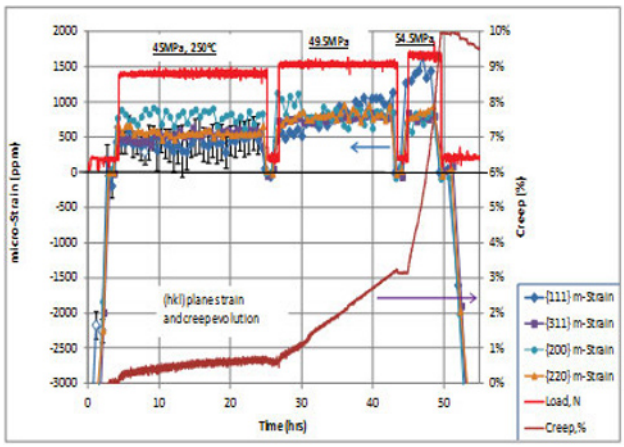

(b)

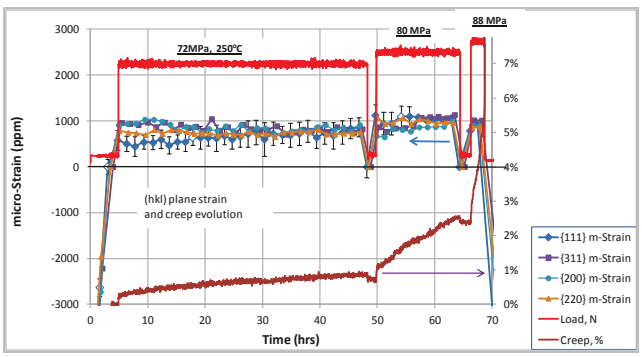

(c)

Figure 4. Creep strain (%) and elastic microstrain (ppm) evolution at selected *hkl* planes at 250°C under ascending cyclic loading for A380 alloy (a), "base" alloy (b), and "new" alloy (c)

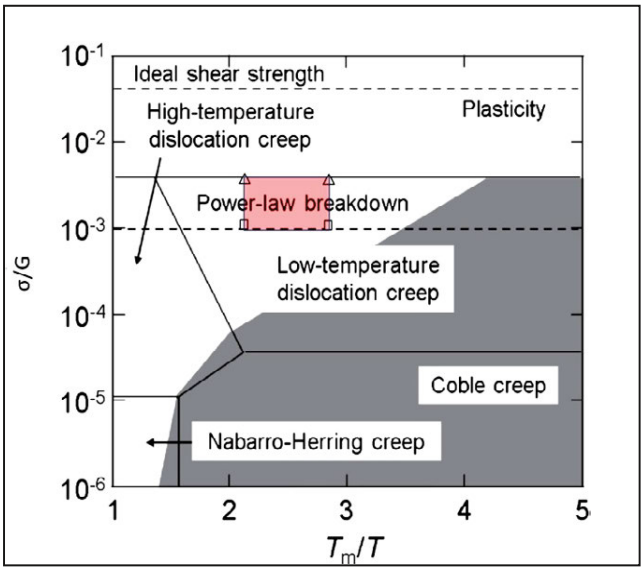

Figure 5. Deformation mechanism map for pure aluminum [3]

Most likely, however, that in the cycling-increasing-load testing conditions of the present study the creep in the tested samples begins as power-law governed dislocation creep and later transitions to PLB creep and finally to plasticity. This hypothesis is supported by the calculated power-law stress exponents (n) for the A380, "base", and "new" alloys, as presented in Figure 6. The governing power-law equation is:

$$\dot{\varepsilon} = A_0\, \sigma^n \exp\left(-\frac{Q}{R\,T}\right), \qquad (3)$$

where $\dot{\varepsilon}$ is the minimum creep rate, 1/s; A_o is dimensionless constant, σ is the applied stress, MPa, Q is the creep activation energy, kJ/mol; R is the universal gas constant, J/(mol K); and T is the absolute temperature, K.

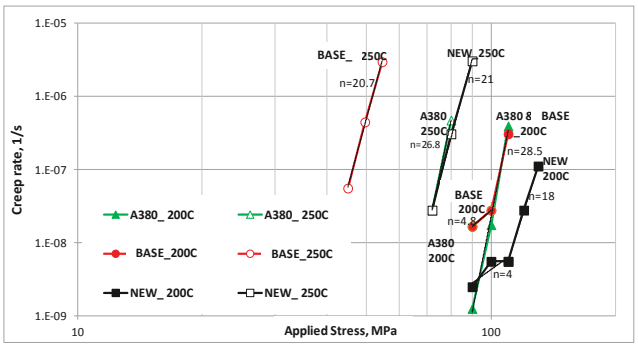

Figure 6. Calculated stress exponents of the tested alloys at the temperatures of 200°C and 250°C

The experiment-based calculated results presented in Figure 6 mostly display large values of stress exponent, typically exceeding 18. According to reference [3], these high values of n represent the PLB creep region, which starts when the value of stress exponent exceeds 5. For $1<n<5$ the creep is characterized by dislocation creep for which the power law (Equation 3) is applicable.

Figure 6 also indicates that there are two exceptions from the typical for this experiment PLB creep ($n>18$): specifically, at the lower temperature of 200°C the "base" alloy exhibited the dislocation power-law creep at applied stresses of 90 and 100 MPa with n =4.8; the "new" alloy performs similarly at the same temperature at applied stresses of 90 and 110 MPa with n=4.

Creep Deformation with Respect to Crystallographic Planes

The experimental results presented in Figure 1 indicate that for the lower temperature of 200°C the load is mostly supported by the (111) and (311) planes, because the measured elastic μ-strains are the largest in the [111] and [311] directions. However, at the higher temperature of 250°C (Figure 2), there is a greater contribution by the (220) and (200) planes to supporting the load.

As reported previously [3], the dislocations can move easier on certain crystallographic planes than on others and in certain preferred crystallographic directions of atoms than in others. The close-packed planes and directions (i.e. the planes and directions having the highest planar and linear atomic packing densities) are the most preferred dislocation slipping planes and directions allowing the dislocations to move easier. In aluminum with its face-centered cubic (FCC) crystal structure, the close-packed planes are (111), which have the highest planar density of 14 atoms/nm^2, and the direction is [110]. The higher planar density of the (111) plane leads to its higher load carrying capacity than the less-packed (220) and (200) planes.

Although the (311) planes have a lower planar density, 8 atoms/nm^2, it also provides a high capacity in supporting the applied load, as shown in Figure 1. This is attributed to the fact that the [311] direction is oriented with difference of just 30° in relation to the [111] direction. The relatively small difference in direction makes the (311) planes able to carry almost the same portion of the load as (111) planes, which is indicated by the similar *hkl* microstrain levels.

During the second and subsequent re-loading steps, the less-packed planes can be activated to carry more of the load, in some cases these planes are strained almost as much as (111) planes. This activation can be attributed to accumulated plastic deformation resulting in grain deformation and re-orientation that may lead to cross-slip from the (111) plane to the (311) and (220) planes. Similar deformation behavior was reported in a previous study [4], in which the cross-slip is activated from the (111) plane onto the (001) planes as the load increases.

Temperature is also a significant factor in the strain. Although FCC metals deform easily by glide on the octahedral planes, such as (111), it is believed that the glide can also take place on less-packed planes such as (220) and (200) at high temperatures. This believe is in agreement with other studies [5-7], which report that above 200°C aluminum deforms easily by glide on the non-

compact family planes of (100), (110), (112) and (113) types and conclude that those planes are thermally activated. The activation enthalpies for less-packed slip planes in aluminum are in the range of 1.2 to 1.9eV depending on which planes are activated [8, 9]. This range agrees with the creep activation enthalpies above 200°C, which range between 1.3 and 1.6eV [8].

It is worth mentioning that the critical resolved shear stress of less-packed planes can be reduced significantly as the temperature increases. For example, in hexagonal close-packed (HCP) metal such as zirconium, the critical resolved shear stress for slip on the $(10\bar{1}0)[\bar{1}2\bar{1}0]$ system is decreased from 10MPa to 0.2MPa, as the temperature increases from 77K to 575K [3]. Accordingly, in the present study the increase of temperature from 200°C to 250°C can result in a significant activation of less-packed crystallographic planes of (220) and (200) enabling them to better support the applied load, as evidenced in Figure 2.

Conclusions

1. Three aluminum alloys have been subjected to *in-situ* creep testing under the high-temperature high-load conditions, typical for automotive powertrain applications. Both total (plastic and elastic) and elastic-only strains have been measured and analyzed. The creep mechanism typical for each stage of incremental loading has been discussed.
2. The main creep mechanism is dislocation creep that starts at the lower load setting that was close to the yield strength and is associated with the power-law-governed creep. As the applied load increased, the creep mode shifted to the power-law breakdown (PLB) that was dominant for most of the testing conditions.
3. For the lower temperature of 200°C the load is mostly supported by the (111) and (311) planes, as the measured elastic μ-strains are the largest in the [111] and [311] directions. These measured strains increase throughout the experiment correlating to the increase in the appplied load. The (220) planes may also become activated, as shown for A380 alloy at 100 MPa.
4. The close-packed planes and directions, eg. {111}, are the most preferred dislocation slipping planes and directions where the dislocations movement is easier. The higher packing density of the {111} planes enable them to better support the applied stress than the less-packed (220) and (200) planes.
5. The [311] direction is only 30° from the [111] direction, and this small angular difference makes the (311) planes able to carry almost the same portion of the load as (111) planes even though the (311) planes have a relatively low planar density.
6. Under certain conditions the less-packed planes can be activated to carry a significant part of the load:
   - accumulated plastic deformation resulting in grains deformation and re-orientation may lead to the cross-slip from (111) to (311) and (220) planes.
   - high temperature may lead to thermal activation of the (200) and (220) glide.
7. The "new" alloy has shown superior performance in conditions simulating an in-service automotive powertrain component, such as an engine head. Its performance was superior in both ultimate strength and total (plastic and elastic) creep, which can be explained in part by activation all the observed *hkl* planes to support the load.

References

1. A.V. Paratwar, D.B Hulwan, "Surface Temperature Prediction and Thermal Analysis of Cylinder Head in Diesel Engine", International Journal of Engineering Research and Applications (IJERA) ISSN: 2248-9622 www.ijera.com, Vol. 3, Issue 4, Jul-Aug 2013, pp.892-902
2. T. Mastsunaga, E. Sato, "Creep Mechanism in Several Grades of Aluminum at Low Temperatures," Materials Transactions, Vol. 54(12), 2013, pp. 2202-2208
3. G.E. Dieter, Mechanical Metallurgy, 3rd Edition, McGraw Hill Publishing Co., 1986, 747 p.
4. J. Majimel, M.-J. Casanove, G. Molenat,"A 2XXX Aluminum Alloy Crept at Medium Temperature: Role of Thermal Activation on Dislocations Mechanisms," Materials Science and Engineering A, Vol. A380, 2004, pp. 110-116
5. D. Caillard, J. L. Martin, "Glide of Dislocations in non-octahedral Planes of FCC Metals: A Review", Int. J. Mat. Res., Vol. 100 (10), 2009, pp. 1403-1410.
6. M. Carrard , J. L. Martin , Philos. Mag.. A 56, 1987, p.391.
7. R. Le Hazif, P. Dorizzi, J. P. Poierier, Acta Met., Vol. 21, 1973, p.903.
8. D. Caillard, J. L. Martin, "Some Aspects of Cross-Slip Mechanisms in Metals and Alloys", J. Phys., Vol. 50, 1989, pp. 2455-2473.
9. J. Bonneville, D. Caillard, M. Carrard, J. L. Martin, "Rate Controlling Processes in Creep of Close Packed Metals at Intermediate and High Temperatures", Revue. Phys. Appl., Vol. 23, 1988, pp. 461-473